Desalination and Water Treatment
www.deswater.com

doi: 10.5004/dwt.2023.29587

294 (2023) 172–184
May

Naturally occurring metal oxides from rocks as capacitive deionization electrode material for antibacterial activities

Furaha Ndeki Alphonce[a,b], Tusekile Alfredy[a,b], Askwar Hilonga[a,b], Yusufu Abeid Chande Jande[a,b,*]

[a]*Department of Material and Energy Science Engineering, The Nelson Mandela African Institution of Science and Technology (NM-AIST), P.O. Box: 447, Arusha, Tanzania, Tel.: +255787303091; emails: yusufu.jande@nm-aist.ac.tz (Y.A.C. Jande), alphoncef@nm-aist.ac.tz (F.N. Alphonce)*
[b]*Water Infrastructure and Sustainable Energy Futures Centre of Excellence, The Nelson Mandela African Institution of Science and Technology, P.O. Box: 447, Arusha, Tanzania, emails: tusekile.alfredy@nm-aist.ac.tz (T. Alfredy), askwar.hilonga@nm-aist.ac.tz (A. Hilonga)*

Received 11 November 2022; Accepted 30 April 2023

ABSTRACT

The present study aimed to investigate the efficacy of activated carbon (AC) electrode embedded with naturally occurring metal oxides (MO) from rocks for antibacterial activities against both gram-negative (*Escherichia coli*) and gram-positive (*Salmonella aureus*) bacteria using capacitive deionization technique. The desalination and disinfection performance of the fabricated AC/MO electrode was evaluated through the batch mode experiments conducted at a potential difference of 1.2 V for 240 min (4 h). The results revealed that the AC/MO electrode achieved a complete removal efficiency of 100% for *E. coli* and 60% for *S. aureus* in the field water collected from Nduruma stream (natural water). The bacterial removal mechanism was attributed to the capacitive deionization (CDI) process and physical adsorption. The study highlights the potential of AC/MO electrode material as an effective antibacterial agent for the CDI process, which may have significant implications for the development of new technologies for water purification and disinfection.

Keywords: Capacitive deionization; Antibacterial; Metal oxides; Activated carbon; Disinfection

1. Introduction

Water demand has increased dramatically because of global population growth, new technological advancement, and agricultural uses for water, but scarcity remains one of the most pressing and consequential challenges of the twenty first century [1]. According to the report published by the World Health Organization (WHO) in 2021, around 2.8 billion people worldwide do not have access to safe and clean water [2]. Clean water means water without any toxic chemicals and pathogens [3]. To date, several techniques such as reverse osmosis (RO), ion-exchange resin (IE), electrodialysis (ED), thermal distillation (TD), thermal-based multi-stage flash (TBMF), and multi-effect distillation (MED) have been employed by researchers for water treatment and purification [4]. Most of these techniques can achieve high water purification efficiency with excellent stability, but have drawbacks including high energy consumption, secondary waste generation, high maintenance cost, and equipment fouling problems [5]. Therefore, to overcome such shortcomings conventional desalination technology is required [6].

Capacitive deionization (CDI) is a promising and rapidly growing technology that is easy to operate, environmentally friendly and energy efficient for brackish water (<10,000 mg/L) desalination [7]. Furthermore, the CDI

* Corresponding author.

technology uses low pressure and non-membrane processes, making it a viable water desalination technique [8]. Water desalination by CDI is based on the principle of electric double layer capacitors (EDLs), whereby the charged ions from the aqueous solution adsorbed and electrostatically stored on the oppositely charged surfaces of electrodes through the application of potential difference from an external source of power [1]. When the external potential difference is removed or reversed, the adsorbed ions released back to the solution, which resulting in the regeneration of electrodes [9]. Chemical and physical properties of electrodes materials play a significant role in capacitive deionization (CDI) performance [10]. To date, different carbon materials have been studied including porous carbon, aerogels, activated carbon, carbon nanotubes, carbon nanofibers, and graphene [11]. These materials has suitable properties including high specific surface area (SSA), good wettability, high adsorption capacity, chemical inertness, high electrical conductivity, suitable pore size distribution, and high capacitance [12].

Capacitive deionization technique has been employed in many investigations to treat water, however the presence of microbes in desalinated water remains a significant challenge. Various antibacterial agents have been used to overcome such problem including hypochlorite, chlorine, peroxides, ozone, and zeolite [13,14] have been used to remove microbes in water, however they were faced with limitations such as production of hazardous by-products that are carcinogenic, mutagenic, highly irritating, and damaging to human health and the environment [15,16]. Recently, activated carbon (AC) loaded with different nanomaterials have been studied in CDI for antibacterial activity including silver nanoparticles (AgNPs) [17], gold nanoparticles (AuNPs) [18], carbon nanotubes (CNTs) [19], and graphene oxide (GO) [11]. Abdallah et al. [20] uses the silver nanoparticles embedded with activated carbon (AC/AgNPs) for antimicrobial activities using CDI and achieved to kill 100% of *Escherichia coli* and 98% of *Salmonella enteritidis* after charging for 3 h during the CDI process, Yasin et al. [21] uses nitrogen doped tin oxide intercalated activated carbon non composite (N-AC/SnO_2) and composite nitrogen-TiO_2/ZrO_2 nanofibers incorporated activated carbon (NACTZ) electrode materials which show good antibacterial effects as well as desalination performance. Wang et al. [22] also uses capacitive deionization disinfection (CDID) electrode made by coating an activated carbon (AC) with cationic non hybrid of graphene oxide-graft-quaternized chitosan (GO-QC), (GO-QC/AC CDID electrode) and achieved to kill 99.9999% (6 log reduction) of *E. coli* in water. Although activated carbon electrodes loaded with nanomaterials are effective on inhibiting bacterial activity in desalinated water, their implementation on a broad scale is challenging due to their high cost, rigid reaction conditions, and challenging fabrication methods [23,24]. Additionally, various studies have reported the toxicity effects of nanomaterials including AgNPs [25], AuNPs [26], CNTs [27], and GO [28] on rat liver and murine stem cells, human nerves, and its poisonous impacts on aquatic organisms in nanomolar concentration. Metal oxides (MO) including TiO_2, ZnO, CuO, SnO_2, and MnO recently attracted special attention due to their unique properties and noticeable effect against bacterial activities in water [29]. Furthermore, MO are renowned for being affordable, plentiful, non-toxic, and eco-friendly [30]. Rocks are naturally occurring materials which containing MO including SiO_2 abundantly [31] which showing appreciable antibacterial activity without use of chemicals and low cost. To the best of our knowledge there have been no studies reported on the use of naturally occurring MO from rocks in the CDI system for antibacterial activities in desalinated water. Therefore, this study aims to replace high-cost antibacterial agents by investigating the naturally occurring MO from rock materials as an alternative low-cost AC/MO electrode with high antibacterial activity in water using the CDI technique. To the best of our knowledge there have been no studies reported on the use of naturally occurring MO from rocks in the CDI system for antibacterial activities in desalinated water.

2. Materials and method

2.1. Materials

Biocontaminated water (natural water) was collected from Nduruma stream located near the institution (Nelson Mandela African Institution of Science and Technology, Arusha-Tanzania), rocks sample collected from Singida Region in Iramba District (Ibaga Village, GPS coordinates 4.19.60S, 34.30.0E), activated carbon powder (purchased from FINAR Co., Ltd.), polytetrafluoroethylene (PTFE) and carbon black (CB), ethanol 100% (purchased from Chem-Lab NV, Belgium), sodium chloride (purchased from Loba Chemie Pvt. Ltd.), Hi chrome *E. coli* agar (purchased from Hi-Media Co. Ltd.), deionized water (DI), and cellulose nitrate filter paper with pore size of 0.45 μm and bismuth sulfite (BSA) media (purchased from Sartorius Stedim Biotech GmbH).

2.2. Synthesis of AC/MO electrodes

The rock sample was washed with deionized water several times to remove some impurities and oven dried at 60°C for 1 h. Then the rock samples were grinded into powder form followed by sieving with a sieve of 180 μm followed with a sieve of 90 μm for removing large particles. The fine powder obtained were used for synthesizing the electrode for CDI technique, in which the rock powder mixed with AC mechanically, together with CB, and PTFE in the ratio of 5:3:1:1, respectively, with ethanol in a beaker of 100 mL and then stirred for 60 min using magnetic stirrer at a temperature of 80°C until all ethanol evaporated and then the dough slurry obtained. Then the obtained slurry was pressed using a presser machine to a specified thickness of 1 mm then cut into 4 cm^2 × 4 cm^2 and oven dried at 60°C overnight to remove the remaining organic solvent. After drying, the real weight of the electrode was measured.

2.3. Characterization of electrode materials

The elements and MO present in the rock material was characterized by X-ray fluorescence (XRF) (EZ5001XSV) and the crystallinity, structure and crystal size of the rock materials was determined by X-ray diffraction (XRD) using a Rigaku (Tokyo, Japan) Miniflex X-ray Diffractometer with Cu-K_α radiation source (λ = 0.15418 nm) at 50 kV and 30 mA,

and reflection geometry at 2θ values range from 5° to 90°. The diffraction peaks were assigned through the comparison with powder diffraction files of Joint Committee on Powder Diffraction Standards (JCPDS). The crystallite average size of the rock material was calculated by using the Scherrer Eq. (1).

$$D = \frac{K\lambda}{\beta\cos\theta} \quad (1)$$

where D is the average crystallite size in nm, k is known as Scherrer's constant, which is 0.94 for spherical crystal, λ is the wavelength, β is the full-width at half maximum (FWHM) of high intensity diffraction peak in radians and θ is the angle of diffraction in degrees.

The surface morphology of AC and AC/MO electrode was examined using the scanning electron microscopy (SEM) coupled with the energy-dispersive X-ray spectroscopy (EDX). The specific surface area of the AC powder was measured based on N_2 adsorption isotherms using BET surface area analyzer. The pore size distribution was obtained by using the Barrett–Joyner–Halenda (BJH) method. The functional groups of AC and AC/MO were investigated using Fourier-transform infrared spectroscopy (FTIR) using Tensor 27 spectrometer fitted with high through-put screening device (HTS-XT). The test was conducted in absorbance mode in spectral range of 4,000–500 cm^{-1}.

2.4. Antibacterial performance through CDI

The antibacterial performance of AC/MO electrode was evaluated in batch mode experiment, the CDI cell comprises of two electrodes arranged parallel to each other and connected with IVIUM STAT (Vertex. 1A. EIS 1A/10V/1MHZ EIS, Ivium Technologies, The Netherlands) together with peristaltic pump as presented in Fig. 1. Then 30 mL of bio contaminated water collected from Nduruma River with an initial conductivity of 405.6 μS/cm was pumped between the two electrodes placed parallel to each other at flow rate of 5 mL/min for 4 h at a potential difference of 1.2 V to the cell. The conductivity of the effluent was recorded after every 10 min.

2.5. Microbes culturing

The membrane filtration (MF) method was used for culturing bacteria, in which 30 mL of field bio-contaminated water was filtered using membrane filter paper (cellulose nitrate filter paper with diameter of 0.45 μm) before and after treatment and the filter paper was subsequently placed onto the surface of Hi chrome *E. coli* agar plates for enumeration of gram-negative bacteria *E. coli*, then another 30 mL of bio-contaminated water was filtered and the filter paper placed onto surface of bismuth sulfite agar (BSA) plates for enumeration of gram-positive bacteria *Salmonella aureus*. The petri dishes were incubated at 37°C for 24 h, the colonies formed were counted using digital colon counter and the percentage removal was determined using Eq. (2) as follows.

$$\text{Bacterial removal} = \left(\frac{A-B}{A}\right)\times 100 \quad (2)$$

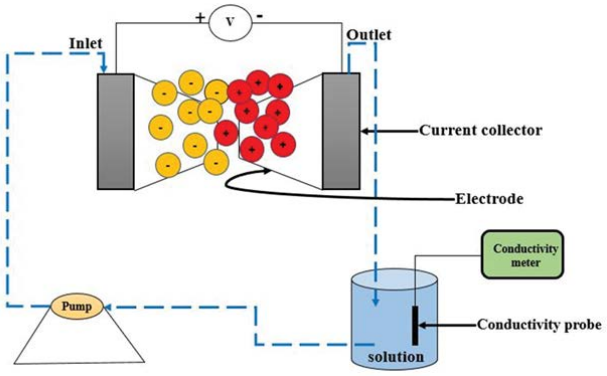

Fig. 1. Schematic diagram of capacitive deionization experiment set-up.

where A = number of microbial viable cells before treatment and B = number of microbial viable cells after treatment.

3. Results and discussion

3.1. XRF and XRD analysis

The X-ray fluorescence (XRF-EZ5001XSV) instrument equipped with Uniquant Software was used for analysis of MO presents in the rock samples. The obtained XRF results reveal that the rocks samples containing higher concentration of silicon dioxide (SiO_2) with a mass composition of 53.25% compared to other metal oxides identified as shown in Table 1.

The crystallinity analysis of the rock samples was investigated by using the XRD. The XRD pattern of the rock materials is shown in Fig. 2. The diffraction peaks at 2θ = 21.34°, 25.57°, 26.59°, 35.45°, 37.90°, 40.02°, 42.76°, 50.78°, 55.45°, 61.38°, 67.38°, 75.63°, 80.42°, and 82.74° are assigned to (223), (110), (101), (002), (240), (200), (220), (211), (103), (215), (222), (202), (104), and (244) crystallographic planes (*hkl*) of K_2O, Al_2O_3, SiO_2, CuO, Fe_2O_3, MgO, Na_2O, MnO, CaO, TiO_2, ZnO, and P_2O_5 which are matched with the JCPDS card number 75-0576. The crystallite average size of the rock material was calculated by using the Scherrer equation [Eq. (1)] and found to be 34.56 nm. The average crystallite size depicts that the rock powders are nano-size which enhance the high surface area of the MO contained in the rock materials against the bacterial activities for both gram-positive (*E. coli*) and gram-negative (*S. aureus*).

3.2. SEM-EDX and transmission electron microscopy analysis

The surface morphology of both AC and AC/MO was characterized by the SEM. The resulting images show rock and rough-like surface of the AC electrode, as depicted in Fig. 3a. These observations suggest that the AC electrode is capable of effectively adsorbing ionic impurities during the deionization process [32]. The SEM image presented in Fig. 3b illustrates that the surface of the fabricated AC/MO electrode exhibits a mesh-like structure composed of hollow tubes. This observation implies the presence of the rock particles containing MO on the surface of AC electrode, which was

Table 1
X-ray fluorescence analysis results of metal oxides and mass composition (%) of rock samples

Metal oxides	Mass composition (%)
SiO_2	51.95
Al_2O_3	15.45
CuO	10.45
Fe_2O_3	9.36
MgO	4.90
Na_2O	1.98
CaO	0.73
TiO_2	0.55
K_2O	0.47
ZnO	0.19
P_2O_5	0.12
MnO	0.006

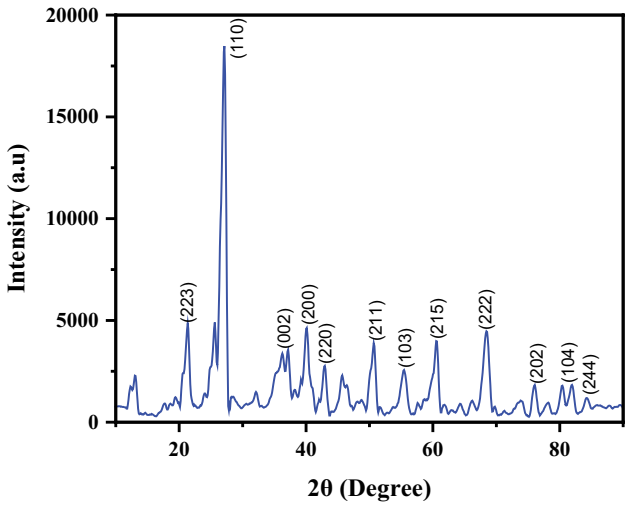

Fig. 2. X-ray diffraction spectra of rock sample containing metal oxides.

further confirmed by the EDX analysis. The particle size and morphology of both synthesized AC/MO electrode and the rock powder containing MO was analyzed using transmission electron microscopy (TEM), as depicted in Fig. 3c and d. The resulting TEM micrographs demonstrate that the A1O electrode is composed of spherical rock particles with average particle size ranging from 20 to 35 nm (Fig. S1), which is consistent with an average particle size estimated using Scherrer equation based on the XRD pattern. The spherical of rock particles containing MO contributes to their increased reactivity, owing to their high surface area-to-volume ratio and high-atom-density surfaces, resulting in heightened antimicrobial activity of AC/MO [33]. Moreover, the positive surface charge of these rock particles facilitates their binding to the negatively charged surfaces of the bacteria, potentially enhancing the bactericidal effects of AC/MO [34]. As reported by [35], the shape of metal oxide nanoparticles (MO-NPs) plays a significant role in their antimicrobial properties as it promotes greater contact with bacterial cells. Hence, the nano size of rock particles containing MO were found to exhibit detectable antibacterial activity during the CDI process.

The elemental composition of AC/MO electrode material was confirmed by the EDX analysis which shows the presence of silicon (43.97%), magnesium (0.66%), aluminum (2.76%), sulphur (0.09%), iron (2.04%), nickel (0.27%), copper (1.52%), zinc (0.25%), and oxygen (47.8%). Fig. S2 displays EDX analysis results of AC, and it can be observed that oxygen (O), silicone (Si), sulfur (S), nickel (Ni), aluminum (Al), chlorine (Cl), and calcium (Ca) were existing in the AC alongside with carbon (C) which indicating the presence of impurities in the AC powder as summarized in Table S1.

3.3. FTIR analysis of AC and AC/MO electrodes

The FTIR analysis was conducted to characterize the functional group present on AC and AC/MO electrode materials and results are presented in Fig. 4. It was observed that AC reveal the strong characteristic wide peak at 3,285 cm^{-1} which is attributed to the stretching vibration of O–H bond, peak at 2,889 cm^{-1} which is attributed to C–H bond, peaks at 2,358 cm^{-1} which is attributed to stretching and vibration of C–OH bond in carboxyl group (COOH) and peak at 1,206 and 1,790 cm^{-1} which is attributed to C–O and C=O bond. On the other hand, AC/MO reveal the strong characteristic wide peak at 3,684 cm^{-1} which is attributed to stretching and bending vibration of O–H bond, peak at 2,093 cm^{-1} attributed to stretching and vibration of C–H bond, peaks at 1,000 and 1,407 cm^{-1} which is attributed to stretching and vibration of C–O and C=O bond. These results shows that the presence of hydrophilic groups such as carboxyl and hydroxyl on the surface of electrodes enhance the wettability and electrosorption capacity of carbon materials [36]. Mohammed et al. [37] reported that the presence of the phenolic and carboxyl functional group have significant effect against the bacterial activities when interacting with the cell membrane of bacteria.

3.4. Antibacterial activity of AC and AC/MO electrodes

Bacteria removal efficiency with CDI in bio-contaminated field water was characterized before treatment and found to have both gram-negative bacteria *E. coli* and gram-positive bacteria *S. aureus*, which were detected as model pathogens in testing antibacterial activities. Fig. 5a–c depicts the gram-negative *E. coli* bacteria before and after subjecting them to treatment with AC and AC/MO electrodes using the CDI technique. Notably, the findings reveal that the application of AC and AC/MO electrodes resulted in a substantial reduction of gram-negative bacteria with the highest bacterial removal rate of 92% and 100%, respectively. Also, Fig. 5d–f shows the gram-positive bacteria *S. aureus* before and after treatment. The experimental results indicate that the use of pristine AC electrode for antibacterial activity resulted in a removal rate of 45%. However, when AC/MO electrodes were employed, a significant improvement in antibacterial activity was observed, as evidenced by a removal rate of 60%. During the disinfection experiment, it was noted that the conductivity of bio-contaminated water (measuring 405.6 μS/cm) underwent a gradual change over

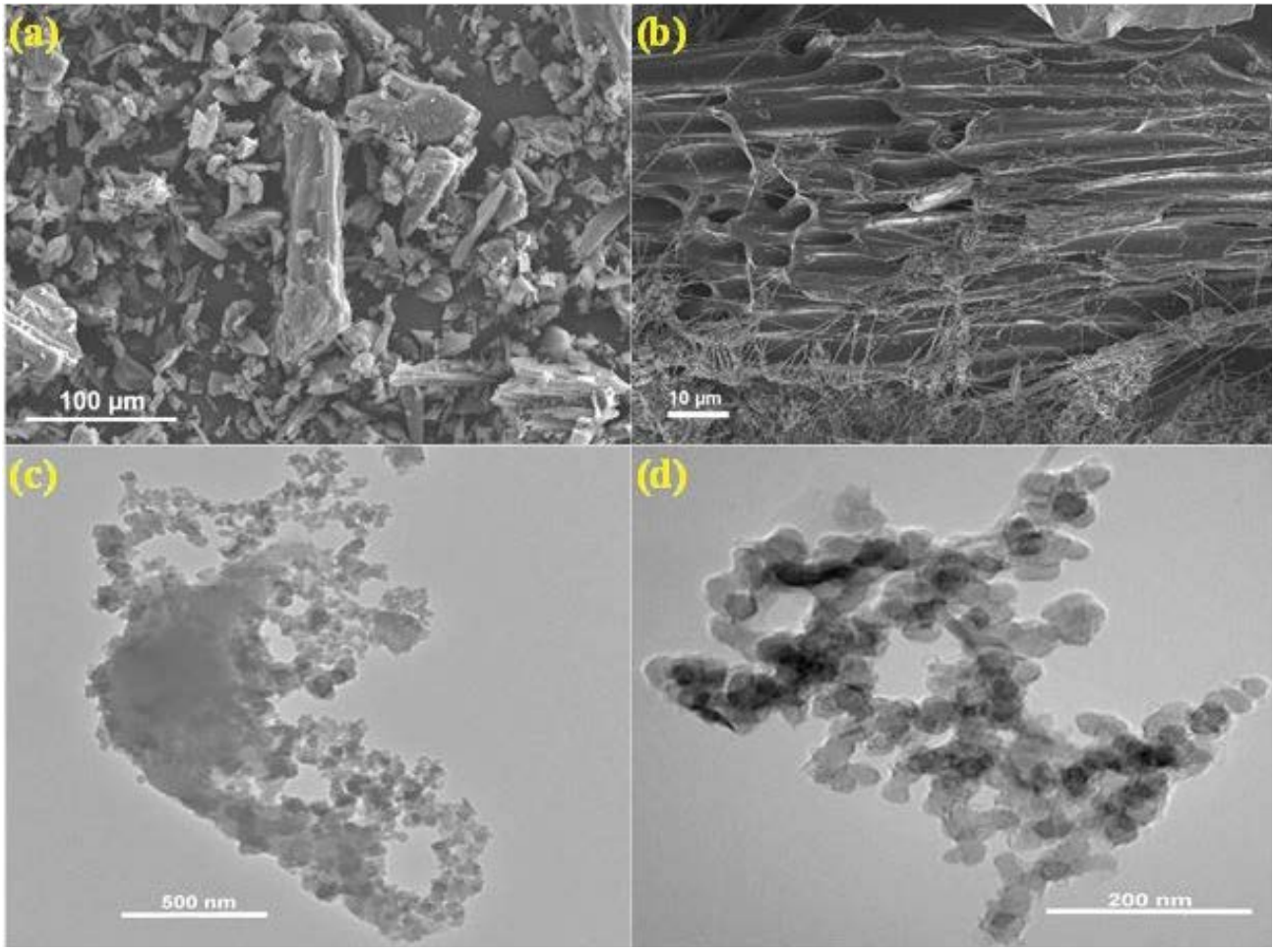

Fig. 3. (a) Scanning electron microscopy of activated carbon electrode structure, (b) SEM of composite AC/MO electrode, (c) transmission electron microscopy of AC/MO electrode and (d) transmission electron microscopy of rock powder containing metal oxides.

time for both AC and AC/MO electrodes as presented in Fig. S3. In the first 60 min, conductivity dropped from 405.6 to 367.3 µS/cm, and 275.2 µS/cm for AC and AC/MO electrodes, then dropped further to 208.4 and 190.7 µS/cm after 180 min and a plateau reached is indicative of electrodes saturation. The observed decline of conductivity suggests that the ions are being adsorbed onto the electrodes possessing an opposite charge under the application of potential difference. Furthermore, removal rate of bacteria along with ions influenced by the presence of negative charges which attributed by thiol (–SH), amino (–NH), and carboxylic (–COOH) group of proteins present on the bacterial cell wall. After subjecting the bio-contaminated water with AC and AC/MO electrodes the results reveal a noteworthy reduction in both gram-positive and gram-negative bacteria (*E. coli* and *S. aureus*). The AC/MO electrodes show the significant antibacterial effect toward both bacteria *E. coli* and *S. aureus*. The removal efficiency of the former was found to be 100%, while that of the latter was determined to be 60%, after 4 h of charging without dilution as compared to AC pristine electrodes (Fig. 6). Furthermore, the antibacterial activity of pure MO electrodes was evaluated against both gram-negative (*S. aureus*) and gram-positive (*E. coli*) bacteria. The highest bacterial removal rate of 100% and 52% were achieved for *S. aureus* and *E. coli*, respectively, after 4 h of charging as depicted in Fig. S4a–f. The findings suggest that MO electrodes exhibit a substantial impact on bacterial activity when compared to pristine AC electrodes. Nevertheless, MO electrodes suffered from leaching effect during the CDI process. The data suggests that the removal rate of *E. coli* bacteria is relatively greater than *S. aureus* bacteria for both AC/MO and MO electrodes. This observation may be attributed to the fact that *E. coli* bacteria possess a thin cell wall structure which is more susceptible to penetration by metal ions from the electrodes and reactive oxygen species (ROS), leading to cell death. In contrast, *S. aureus* has a thick peptidoglycan layer which provides a greater degree of resistance against the penetration of metal ions and ROS.

3.5. Bacterial removal mechanism during CDI process

During the charging process in CDI, the bacteria were electrically attracted towards the positive electrode due to the presence of negative charges attributed by thiol (–SH), amino (–NH) and carboxylic (–COOH) groups of proteins present on their cell wall and then killed by the embedded metal

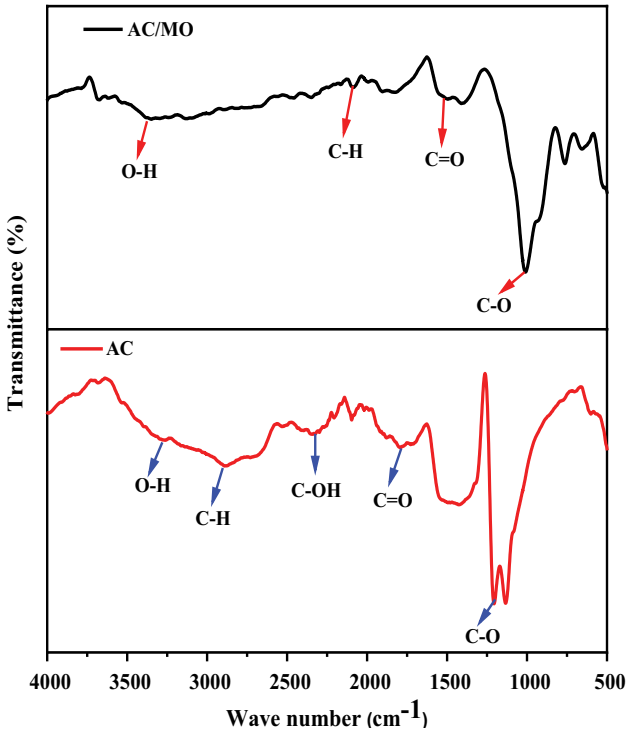

Fig. 4. Fourier-transform infrared spectra of pristine activated carbon and AC/MO electrodes.

oxides from the rocks by physical contact [38]. The effectiveness of metal oxides against antibacterial activities was due to the release of metal ions and regeneration of ROS (Fig. 7). The released metal ions interact with membranes proteins which leading to a drastic change in the permeability of the membrane through the degradation of lipopolysaccharide resulting to the intracellular leakage which causing the death of bacterial cell and also the metal ions released interact with nucleic acid which preventing replication of DNA and translation process which leading to the death of bacterial cell [39]. Additionally, the released ions from metal oxide reduced to metal atoms by thiol group (–SH) present in enzymes and proteins which inactivating vital proteins blocking, limiting respiration and ultimately leading to the cell death [40]. The ROS generated by metal oxides (MO) in aqueous solution including singlet oxygen (O_2), hydroxyl radical (OH^-) and the superoxide (O_2^-) radical interact with the vital cell biomolecules like polyunsaturated fatty acids (PUFA), proteins, nucleic acids, and carbohydrate to a lesser extent. ROS induces severe oxidative stress and damage to the cell's macromolecules which overall cause lipids peroxidation, alteration of proteins, inhibition of enzymes and RNA/DNA damage [41]. This severe oxidative stress also forms holes or pits within the bacterial membrane which alter the intrinsic membrane properties like fluidity and lysis of bacterial cells which leading to death of microbial cell [42,43].

Furthermore, bacteria cell death could be due to cell wall rupture upon exposure to the high electric field generated

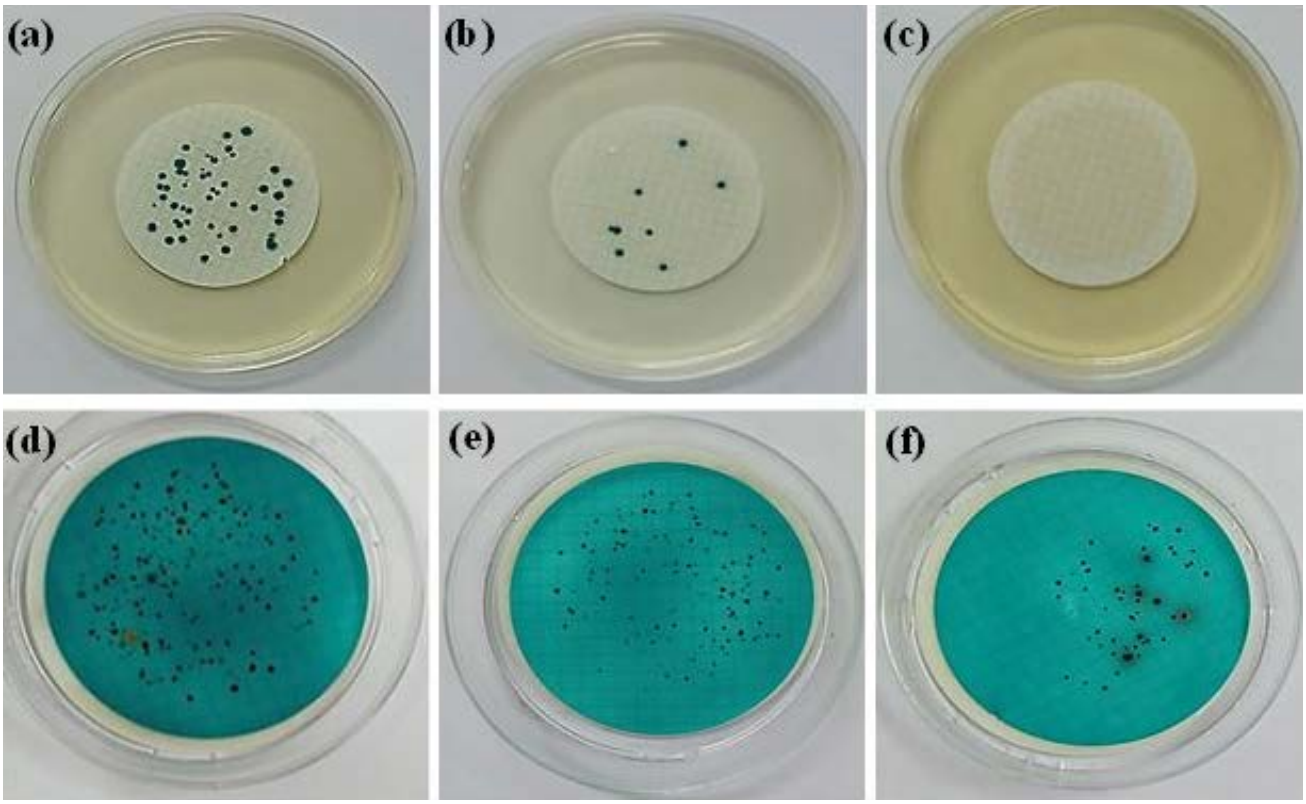

Fig. 5. Plates showing bacteria growth (a,d) before treatment, (b,e) treated with activated carbon electrode, (c,f) treated with AC/MO electrode (Blue colonies indicates *Escherichia coli* and black colonies indicates *S. aureus*).

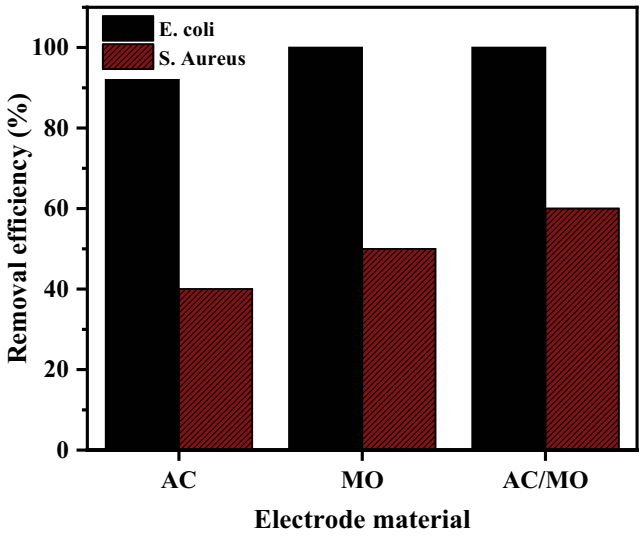

Fig. 6. Bacterial removal efficiency during capacitive deionization process.

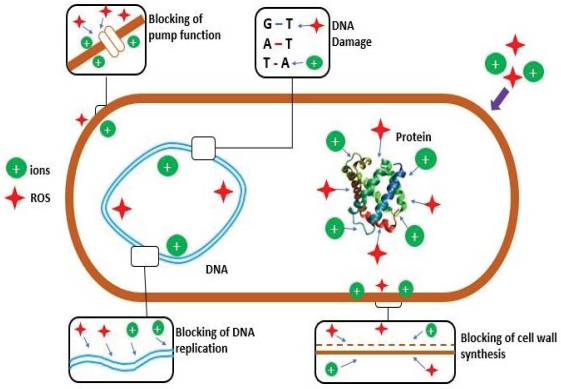

Fig. 7. Effects of metal ions (M^{n+}) and reactive oxygen species on the bacterial cell.

between the electrodes during CDI process [44]. Bacterial cell wall has negative charge due to the presence of phosphates and lipopolysaccharides [45] which can be electrosorbed onto the positive electrode (anode) [46] along with anions, bringing them into proximity to each other. The high concentration of anions in the vicinity at the electrode surface creates a hypertonic environment which leading to dehydration of bacterial cell and eventually leading to cell death of bacteria [47]. Thus, bacterial removal during the CDI process could be due to electro-adsorption of bacteria cell (temporary reduction) or cell death (permanent reduction). To better understand the mechanism the AC/MO electrode was washed with ultrapure water to facilitates removal of any electro-adsorbed bacteria cell on the electrode surface without application of the potential difference on CDI cell, and the effluent was filtered with cellulose membrane filter paper with pore size of 0.45 μm and cultured for bacterial growth. The results (Fig. 8) showed that the number of bacteria colonies formed was lower than that examined prior to the CDI process, which indicating that some of bacteria cells were just electro-adsorbed onto electrode surface, and some were permanently killed due to high concentrations of anions released from the MO during CDI process.

The gram-negative bacteria (*E. coli*) having thin cell wall which can be affected easily by the ions released by the metal oxides (MO) in physical contact and electric field generated during the CDI process, hence being killed for 100% [41] and on the other hand gram-positive bacteria (*S. aureus*) were not removed to 100% due to the presence of the hard thick peptidoglycan layer which prevent easy penetration of metal oxide ions released from the electrode (AC/MO) [48].

3.6. Antibacterial assay of AC and AC/MO by physical adsorption

The AC electrodes were observed to remove bacteria by adsorption, resulting in removal rate of 92% and 30% for *E. coli* and *S. aureus*, respectively. In contrast, the MO and AC/MO were found to be capable of removing bacteria through physical contact without application of the potential difference during the CDI process as illustrated

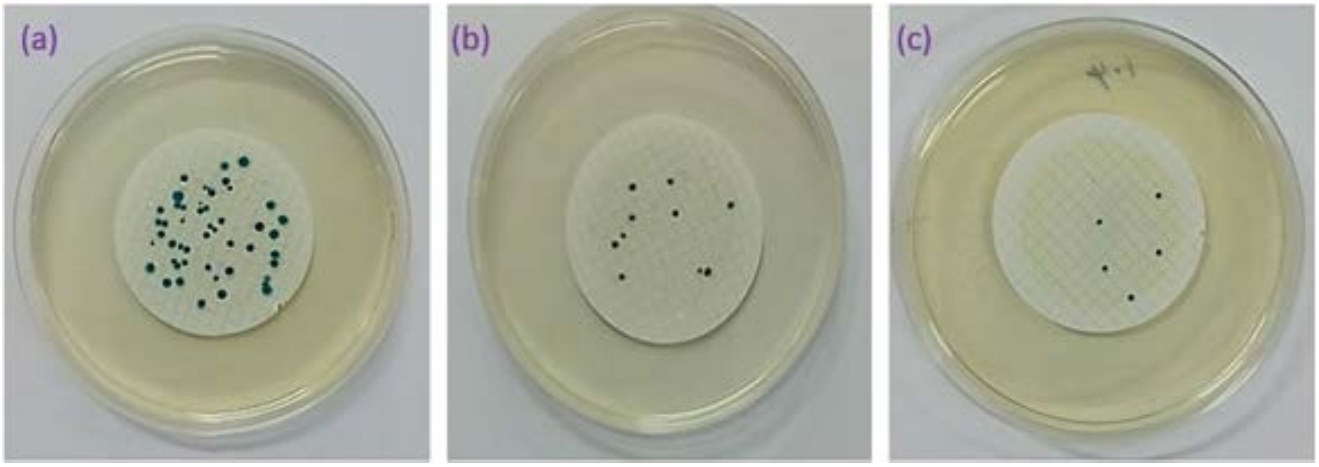

Fig. 8. Plates showing bacteria growth (a) before capacitive deionization and (b,c) bacteria colonies formed when AC/MO electrode washed with ultrapure water without applying voltage in capacitive deionization cell.

in Fig. 9. Following the culturing process, it was observed that the bacteria that had been in contact with AC/MO material did not exhibit any growth on agar plates. Conversely, the bacteria that had been in contact with AC displayed a noticeable growth. This demonstrates that using simply AC may shorten the lifespan of a CDI stack because the bacteria do not perish within the CDI cell.

3.7. Effects of salt concentration on bacteria removal

The concentration of salts ions in bio-contaminated water was analyzed prior to experiment using the flame photometer (FP 6440) in which 14.54 mg/L for Na^+, 41.05 mg/L for K^+, 37.97 mg/L for Ca^{2+} and 33.60 mg/L for Mg^{2+} were determined, respectively, as shown in Table 2. The total concentration of the salt ions in the solution was 246.95 mg/L. However, it was observed that this concentration had no appreciable effects on the death of bacteria during the CDI process. This observation can be attributed to the fact that salinity is one the factors that facilitate bacteria growth, and the ideal concentration of salt for bacteria to survive typically ranges between 200–500 mg/L [49,50]. Therefore, the presence of MO has a significant impact on the disinfection of saline water, as it can effectively reduce the number of bacteria present in bio-contaminated water.

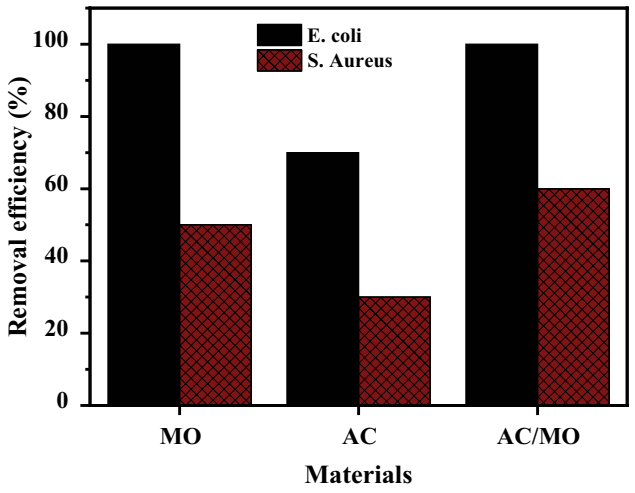

Fig. 9. Bacterial removal efficiency by physical adsorption.

Recent CDI-AC electrode materials present in literatures for water desalination and disinfection are summarized in Table 3.

From the Table 3, it is observed that Cao et al. [54] used cobalt benzimidazole framework (ZIF-9) derived carbon composite with unique quasi-microcubic as an electrode for desalination and antimicrobial activities using CDI and achieved to kill 95% of *E. coli* after charging for 3 h during the CDI process, Janpoora et al. [55] used graphene oxide dendrimer-silver coated electrode (AC/GO/G5/Ag) for water desalination and disinfection using CDI technology and achieved to kill 99.9% *E. coli* bacteria as well as desalination efficiency of 80%. Laxman et al. [56] also used activated carbon cloth (ACC) electrode with electrosorption capacity of 10.5 mg/g and achieved to remove salt for 32% as well as killing 66% of *E. coli* during the CDI process. El-Deen et al. [57] using microporous activated 3D graphene electrode (3DAPGr) with electrosorption capacity of 18.43 mg/g water disinfection via CDI and achieved to kill 98.55% of *E. coli*. Also, Liu et al. used polydopamine hexamethylene guanidine co-deposited activated carbon electrode (AC-PDA/PHMG) with electrosorption capacity of 10 mg/g and achieved to remove 99.11% *E. coli* and 98.67% *Pseudomonas aeruginosa* using CDI. This study used an electrode developed using rock powders that containing MO (AC/MO) and achieved to completely kill 100% *E. coli* (gram-negative bacteria) and 60% *S. aureus* (gram-positive bacteria) after 4 h of charging without dilution of the original sample during the CDI process.

3.8. Effects of applied voltage

The effects of different voltages (0.6, 0.8, 1.0 and 1.2 V) applied during the CDI process on the bacterial removal (*E. coli* and *S. aureus*) were studied using the AC/MO electrode. The 30 mL of bio-contaminated water was filtered using a cellulose membrane filter paper with pore size of 0.45 μm for enumerating the number of microbes before and after the CDI process for both gram-positive and gram-negative bacteria. Fig. S5 shows that effective removal of bacteria was

Table 2
Ionic concentration of field water (C_o), ionic radius (IR), hydration radius (HR), removal efficiency (η) and salt adsorption capacity (SAC)

Ion type	C_o (mg/L)	V	IR[a,b] (pm)	HR[c] (pm)	η (%)		SAC (mg/g)	
					AC	AC/MO	AC	AC/MO
Na^+	14.54	+1	116	358	96	43	0.69	0.26
K^+	41.05	+1	133	331	82	36	1.66	0.60
Ca^{2+}	37.97	+2	65	428	39	30	0.74	0.36
Mg^{2+}	33.60	+2	86	412	46	27	0.78	0.37
PO_4^{3-}	0.34	–3	223	339	74	50	0.012	0.07
NO_3^-	19.20	–1	264	335	81	51	0.77	0.40
Cl^-	0.25	–1	332	332	60	24	0.7	0.002

[a,b,c]References [51–53]

Table 3
Salt and bacterial removal efficiency and electrosorption capacity reported in the literature and findings of this study

Electrode material	Volt (V)	Flow rate (mL/min)	Initial concentration (mg/L)	Salt removal efficiency (%)	Electrosorption capacity (mg/g)	Bacterial removal (%)	References
AC/ZIF-9	1.2	5	584	78	55.4	95 *Escherichia coli*	[54]
AC/GO/G5/Ag	1.2	30	500	80	46.29	99.9 *Escherichia coli*	[55]
ACC	1.6	10	1,000	32	10.5	66 *Escherichia coli*	[56]
3DAPGr	1.4	20	300	75	18.43	98.55 *Escherichia coli*	[57]
AC-PDA/PHMG	1.2	10	250	76	10	99.11 *Escherichia coli* 98.67 *Pseudomonas aeruginosa*	[14]
AC	1.2	5	246.95	62.40	6.21	92 *Escherichia coli* 30 *S. aureus*	This study
AC/MO	1.2	5	246.95	52.85	4.34	100 *Escherichia coli* 60 *S. aureus*	This study

increased as the voltage increased from 0.6 to 1.2 V. The *E. coli* bacteria were removed for 40% at 0.6 V and was increased further to 100% at a potential difference of 1.2 V, but *S. aureus* bacteria were removed for 5% at 0.6 V and increased to 60% at a potential difference of 1.2 V. This depicts that *S. aureus* bacteria cannot be effectively removed at lower potential differences during CDI process in comparison to gram-negative bacteria. This is attributed to the presence of thick peptidoglycan layer on cell wall of *S. aureus*, which resist the electrostatic force and limits the penetration of metal ions and ROS released from AC/MO electrodes during charging process in CDI system [58]. The *E. coli* bacteria were observed to be completely removed to 100%, which could be attributed to presence of thin cell wall composed of lipopolysaccharides that impart a strong zeta potential ranging from –23 to –50 mV. This significant zeta potential can greatly aid their migration toward the positive electrode surface [59].

3.9. Effects of charging time

The impact of varying contact time on the removal of bacteria was studied using bio-contaminated water with a concentration of 246.5 mg/L. The 30 mL of natural water was passed through the CDI cell at a potential difference of 1.2 V at different intervals of time ranging from 60 to 240 min. The findings revealed a positive correlation between charging time and bacterial removal, with increasing charging time leading to a higher removal rate. Specifically, the highest removal rate of 80% for *E. coli* bacteria was attained after a charging time of 3 h during the CDI process, while a removal rate of 30% was achieved for *S. aureus* bacteria following the same charging time. Upon extending the charging time to 4 h, the bacteria removal rate increased to 100% for *E. coli* and 60% for *S. aureus* bacteria. The results presented in Table 4 demonstrate that as the charging time was increased, the rate of bacteria removal increased for both gram-negative and gram-positive bacteria. Therefore, it can be concluded that the charging time has a significant impact of the CDI system in removal of bacterial contaminants.

During the CDI process, the positive and negative charges present on the cell wall of gram-positive and gram-negative bacteria mediate their adsorption onto the oppositely charged electrode surface through electrosorption processes. The interactions of temporary ROS generated from MO increases with an increase in charging time, resulting in oxidative stress on the cell walls, and ultimately leading to cell death [60]. Additionally, the electric field generated during the CDI process may also affect the electrosorbed bacterial cells [61].

3.9.1. Leaching experiment

To investigate the optimal leaching of the metal ions from the electrodes into water, 30 mL of ultrapure water was circulated through the CDI cell containing the electrodes fabricated with the rock powders containing MO exclusively, and that made with the activated carbon (AC/MO) for 4 h of charging without dilution at a potential difference of 1.2 V and flow rate of 5 mL/min. The presence of potential metal ions in water from the rock powder electrodes during the CDI process was analyzed using the atomic absorption spectroscopy (AAS). The obtained results, as presented in Table 5, indicated a significant leaching of metal ions in high concentrations for the electrodes made solely with rock powders. Conversely, the leaching concentration of metal ions was significantly reduced for the electrodes composed of activated carbon and rock powder (AC/MO). This observation suggests that the addition of activated carbon to the electrode synthesis process can result in a substantial reduction of metal ions leaching in the CDI process. The concentration of leached metal ions from the electrodes was compared against the standard guideline established by WHO. The findings reveal that the concentration of leached metal ions from the electrodes made solely with rock powders (MO) exceeded the recommended limit set by WHO. In contrast, the concentration of leached metal ions from AC/MO electrodes was within the acceptable limits established by WHO. The incorporation of AC and MO during the synthesis of electrodes

Table 4
Effects of charging time on bacterial removal rate during capacitive deionization process at 1.2 V

Charging time (h)	Bacteria removal rate (%)	
	Escherichia coli	*S. aureus*
1	30	10
2	50	20
3	80	30
4	100	60

Table 5
Concentration of metals leached in 4 h of charging without dilution at 1.2 V

Elements	Symbol	Concentration (mg/L)		WHO standards (mg/L)
		MO	AC/MO	
Aluminum	Al	0.877	0.078	0.2
Calcium	Ca	4.00	3.60	*
Copper	Cu	3.44	0.29	2
Iron	Fe	1.73	0.06	0.3
Magnesium	Mg	3.36	0.09	*
Manganese	Mn	0.92	0.01	0.1
Nickel	Ni	2.88	0.009	0.07
Potassium	K	82.09	16.34	*
Silicon	Si	9.60	1.265	*
Sodium	Na	2.00	0.077	20
Titanium	Ti	8.30	0.28	*
Zinc	Zn	7.20	0.03	3

Reference [2] (*Not found).

could help to reduce potential health risks associated with metal ions leaching in water during the CDI process.

4. Conclusion

In this study, MO contained in the rock samples has been embedded in AC and used as the electrode for the removal of microbes via CDI application. The MO was found to be an appreciable disinfectant and significantly can remove microbes by physical adsorption as well as during the CDI process against both gram-negative and gram-positive bacterial species (*E. coli* and *S. aureus*). The fabricated AC/MO electrode was tested for antimicrobial performance and was able to remove 100% *E. coli* and 60% *S. aureus* bacteria after charging for 4 h at a potential difference of 1.2 V. Compared to pristine AC, the AC/MO electrode demonstrated superior disinfection capabilities against both gram-positive (*S. aureus*) and gram-negative (*E. coli*) bacteria strains. The findings suggest that the AC/MO composite electrode has potential as an effective antibacterial agent for CDI applications, offering a fast, continuous, and straightforward bacteria contact killing process that does not require complex infrastructure. Therefore, this study presents a novel AC/MO composite electrode material with potential as a substantial antibacterial agent for the CDI processes, with implications for various disinfection applications.

Acknowledgements

The work was carried out with the financial support of the icipe-World Bank Financing Agreement No. D347-3A and the World Bank-Korea Trust Fund Agreement No. TF0A8639 for the PASET Regional Scholarship and Innovation Fund and the authors, also, would like to acknowledge the Catholic Scholarship Program for Tanzania (CSPT) for financial support.

References

[1] N. Zouli, Ceria-incorporated activated carbon composite as electrode material for capacitive deionization, Int. J. Electrochem. Sci, 17 (2022) 22042, doi: 10.20964/2022.04.02.
[2] WHO, Progress on Household Drinking Water, Sanitation and Hygiene 2000–2020: Five Years Into the SDGs, World Health Organization, Geneva, 2021.
[3] N. Savage, M.S. Diallo, Nanomaterials and water purification: opportunities and challenges, J. Nanopart. Res., 7 (2005) 331–342.
[4] M.W. Saleem, Y. Jande, M. Asif, W.-S. Kim, Hybrid CV-CC operation of capacitive deionization in comparison with constant current and constant voltage, Sep. Sci. Technol., 51 (2016) 1063–1069.
[5] P. Díaz, Z. González, M. Granda, R. Menéndez, R. Santamaría, C. Blanco, Evaluating capacitive deionization for water desalination by direct determination of chloride ions, Desalination, 344 (2014) 396–401.
[6] R. Chen, T. Sheehan, J.L. Ng, M. Brucks, X. Su, Capacitive deionization and electrosorption for heavy metal removal, Environ. Sci. Water Res. Technol., 6 (2020) 258–282.
[7] M.E. Suss, S. Porada, X. Sun, P.M. Biesheuvel, J. Yoon, V. Presser, Water desalination via capacitive deionization: what is it and what can we expect from it?, Energy Environ. Sci., 8 (2015) 2296–2319.
[8] T. Yan, J. Liu, H. Lei, L. Shi, Z. An, H.S. Park, D. Zhang, Capacitive deionization of saline water using sandwich-like nitrogen-doped graphene composites via a self-assembling strategy, Environ. Sci. Nano, 5 (2018) 2722–2730.
[9] S. Ahualli, G.R. Iglesias, Á.V. Delgado, Chapter 8 – Principles and Theoretical Models of CDI: Experimental Approaches, S. Ahualli, Á.V. Delgado, Eds., Interface Science and Technology, Granada, Vol. 24, 2018, pp. 169–192.
[10] J. Han, L. Shi, T. Yan, J. Zhang, D. Zhang, Removal of ions from saline water using N, P co-doped 3D hierarchical carbon architectures via capacitive deionization, Environ. Sci. Nano, 5 (2018) 2337–2345.
[11] G. Folaranmi, M. Bechelany, P. Sistat, M. Cretin, F. Zaviska, Comparative investigation of activated carbon electrode and a novel activated carbon/graphene oxide composite electrode for an enhanced capacitive deionization, Materials, 13 (2020) 5185, doi: 10.3390/ma13225185.
[12] K. Rambabu, G. Bharath, A. Hai, S. Luo, K. Liao, M.A. Haija, F. Banat, M. Naushad, Development of watermelon rind derived activated carbon/manganese ferrite nanocomposite for cleaner desalination by capacitive deionization, J. Cleaner Prod., 272 (2020) 122626, doi: 10.1016/j.jclepro.2020.122626.
[13] M. Takayama, Antimicrobial product and antimicrobial agent; Kokin seihin to kokinzai no sayo, J. Petrotech., 21 (1998) 63–68.
[14] N. Liu, P. Ren, A. Saleem, W. Feng, J. Huo, H. Ma, S. Li, P. Li, W. Huang, Interfaces, simultaneous efficient decontamination of bacteria and heavy metals

via capacitive deionization using polydopamine/polyhexamethylene guanidine co-deposited activated carbon electrodes, ACS Appl. Mater. Interfaces, 13 (2021) 61669–61680.
[15] M. Diana, Disinfection by-products potentially responsible for the association between chlorinated drinking water and bladder cancer: a review, Water Res., 162 (2019) 492–504.
[16] D. Stalter, Fingerprinting the reactive toxicity pathways of 50 drinking water disinfection by-products, Water Res., 91 (2016) 19–30.
[17] S. Tang, J. Zheng, Antibacterial activity of silver nanoparticles: structural effects, Adv. Healthcare Mater., 7 (2018) e1701503, doi: 10.1002/adhm.201701503.
[18] S. Sathiyaraj, G. Suriyakala, A. Dhanesh Gandhi, R. Babujanarthanam, K.S. Almaary, T.-W. Chen, K. Kaviyarasu, Biosynthesis, characterization, and antibacterial activity of gold nanoparticles, J. Infect. Public Health, 14 (2021) 1842–1847.
[19] M.K.A. Mohammed, M.R. Mohammad, M.S. Jabir, D.S. Ahmed, Functionalization, characterization, and antibacterial activity of single wall and multi wall carbon nanotubes, IOP Conf. Ser.: Mater. Sci. Eng., 757 (2020) 012028, doi: 10.1088/1757-899X/757/1/012028.
[20] A.S. Abdallah, Y.A. Jande, R.L. Machunda, Evaluation of anti-microbial activities of silver nanoparticles embedded in capacitive deionization electrodes, Desal. Water Treat., 163 (2019) 206–215.
[21] A.S. Yasin, J. Jeong, I.M.A. Mohamed, C.H. Park, C.S. Kim, Fabrication of N-doped &SnO_2-incorporated activated carbon to enhance desalination and bio-decontamination performance for capacitive deionization, J. Alloys Compd., 729 (2017) 764–775.
[22] Y. Wang, A.G. El-Deen, P. Li, B.H. Oh, Z. Guo, M.M. Khin, Y.S. Vikhe, J. Wang, R.G. Hu, R.M. Boom, High-performance capacitive deionization disinfection of water with graphene oxide-graft-quaternized chitosan nanohybrid electrode coating, ACS Nano, 9 (2015) 10142–10157.
[23] Y.-X. Hou, H. Abdullah, D.-H. Kuo, S.-J. Leu, N.S. Gultom, C.-H. Su, A comparison study of SiO_2/nano metal oxide composite sphere for antibacterial application, Compos. B. Eng., 133 (2018) 166–176.
[24] H. Yoon, J. Lee, T. Min, G. Lee, M. Oh, High performance hybrid capacitive deionization with a Ag-coated activated carbon electrode, Environ. Sci. Water Res. Technol., 7 (2021) 1315–1321.
[25] M.C. Stensberg, Q. Wei, E.S. McLamore, D.M. Porterfield, A. Wei, M.S. Sepúlveda, Toxicological studies on silver nanoparticles: challenges and opportunities in assessment, monitoring and imaging, Nanomedicine, 6 (2011) 879–898.
[26] A. Albanese, W.C.W. Chan, Effect of gold nanoparticle aggregation on cell uptake and toxicity, ACS Nano, 5 (2011) 5478–5489.
[27] C. Cheng, Toxicity and imaging of multi-walled carbon nanotubes in human macrophage cells, Biomaterials, 30 (2009) 4152–4160.
[28] M.C. Duch, Minimizing oxidation and stable nanoscale dispersion improves the biocompatibility of graphene in the lung, Nano Lett., 11 (2011) 5201–5207.
[29] M.S. Chavali, M.P. Nikolova, Metal oxide nanoparticles and their applications in nanotechnology, SN Appl. Sci., 1 (2019) 607, doi: 10.1007/s42452-019-0592-3.
[30] J. Sawai, T. Yoshikawa, Quantitative evaluation of antifungal activity of metallic oxide powders (MgO, CaO and ZnO) by an indirect conductimetric assay, J. Appl. Microbiol., 96 (2004) 803–809.
[31] B. Tian, Y. Liu, Antibacterial applications and safety issues of silica-based materials: a review, Int. J. Appl. Ceram. Technol., 18 (2021) 289–301.
[32] T. Tay, S. Ucar, S. Karagöz, Preparation and characterization of activated carbon from waste biomass, J. Hazard. Mater., 165 (2009) 481–485.
[33] M. Guzman, J. Dille, S. Godet, Synthesis and antibacterial activity of silver nanoparticles against gram-positive and gram-negative bacteria, Nanomed. Nanotechnol. Biol. Med., 8 (2012) 37–45.
[34] J.T. Seil, T.J. Webster, Antimicrobial applications of nanotechnology: methods and literature, Int. J. Nanomed., 7 (2012)2767–2781.
[35] S.M. Dizaj, Antimicrobial activity of the metals and metal oxide nanoparticles, Mater. Sci. Eng., C, 44 (2014) 278–284.
[36] L. Chang, Y. Yu, X. Duan, W. Liu, Capacitive deionization performance of activated carbon electrodes prepared by a novel liquid binder, Sep. Sci. Technol., 48 (2012) 359–365.
[37] S.J. Mohammed, H.H.H. Amin, S.B. Aziz, A.M. Sha, S. Hassan, J.M. Abdul Aziz, H.S. Rahman, Structural characterization, antimicrobial activity, and *in vitro* cytotoxicity effect of black seed oil, Evidence-Based Complementary Altern. Med., 2019 (2019) 6515671, doi: 10.1155/2019/6515671.
[38] L. Shkodenko, I. Kassirov, E. Koshel, Metal oxide nanoparticles against bacterial biofilms: perspectives and limitations, Microorganisms, 8 (2020) 1545, doi: 10.3390/microorganisms8101545.
[39] V. Stanić, S.B. Tanasković, Chapter 11 – Antibacterial Activity of Metal Oxide Nanoparticles, S. Rajendran, A. Mukherjee, T.A. Nguyen, C. Godugu, R.K. Shukla, Eds., Nanotoxicity: Prevention and Antibacterial Applications of Nanomaterials Micro and Nano Technologies, Serbia, 2020, pp. 241–274.
[40] A. Raghunath, E. Perumal, Metal oxide nanoparticles as antimicrobial agents: a promise for the future, Int. J. Antimicrob. Agents, 49 (2017) 137–152.
[41] K. Gold, B. Slay, M. Knackstedt, A.K. Gaharwar, Antimicrobial activity of metal and metal-oxide based nanoparticles, Adv. Ther., 1 (2018) 1700033, doi: 10.1002/adtp.201700033.
[42] W. Zhang, Y. Li, J. Niu, Y. Chen, Photogeneration of reactive oxygen species on uncoated silver, gold, nickel, and silicon nanoparticles and their antibacterial effects, Langmuir, 29 (2013) 4647–4651.
[43] S. Dahiya, A. Singh, B.K. Mishra, Capacitive deionized hybrid systems for wastewater treatment and desalination: a review on synergistic effects, mechanisms and challenges, Chem. Eng. J., 417 (2021) 128129, doi: 10.1016/j.cej.2020.128129.
[44] C.-H. Hou, C.-Y. Huang, A comparative study of electrosorption selectivity of ions by activated carbon electrodes in capacitive deionization, Desalination, 314 (2013) 124–129.
[45] D. Deng, W. Aouad, W.A. Braff, S. Schlumpberger, M.E. Suss, M.Z. Bazant, Water purification by shock electrodialysis: deionization, filtration, separation, and disinfection, Desalination, 357 (2015) 77–83.
[46] Y. Oren, H. Tobias, A. Soffer, Removal of bacteria from water by electroadsorption on porous carbon electrodes, Bioelectrochem. Bioenerg., 11 (1983) 347–351.
[47] T. Kristian Stevik, A. Kari, G. Ausland, J. Fredrik Hanssen, Retention and removal of pathogenic bacteria in wastewater percolating through porous media: a review, Water Res., 38 (2004) 1355–1367.
[48] D. Paul, S. Mangla, S. Neogi, Antibacterial study of CuO-NiO-ZnO trimetallic oxide nanoparticle, Mater. Lett., 271 (2020) 127740, doi: 10.1016/j.matlet.2020.127740.
[49] B. Chapman, T. Ross, *Escherichia coli* and *Salmonella enterica* are protected against acetic acid, but not hydrochloric acid, by hypertonicity, Appl. Environ. Microbiol., 75 (2009) 3605–3610.
[50] D.A. Lytle, Electrophoretic mobilities of *Escherichia coli* O157:H7 and wild-type *Escherichia coli* strains, Appl. Environ. Microbiol., 65 (1999) 3222–3225.
[51] B. Tansel, Significance of thermodynamic and physical characteristics on permeation of ions during membrane separation: hydrated radius, hydration free energy and viscous effects, Sep. Purif. Technol., 86 (2012) 119–126.
[52] R. Uwayid, E.N. Guyes, A.N. Shocron, J. Gilron, M. Elimelech, M.E. Suss, Perfect divalent cation selectivity with capacitive deionization, Water Res., 210 (2022) 117959, doi: 10.1016/j.watres.2021.117959.
[53] G.-H. Huang, T.-C. Chen, S.-F. Hsu, Y.-H. Huang, S.-H. Chuang, Capacitive deionization (CDI) for removal of phosphate from aqueous solution, Desal. Water Treat., 52 (2014) 759–765.
[54] S. Cao, T. Chen, S. Zheng, Y. Bai, H. Pang, High-performance capacitive deionization and killing microorganism in

surface-water by ZIF-9 derived carbon composites, Small Methods, 5 (2021) 2101070, doi: 10.1002/smtd.202101070.
[55] F. Janpoora, A. Torabiana, H.A. Panahib, M. Baghdadia, Capacitive deionization and disinfection of water using graphene oxide-dendrimer-silver coated electrodes, Desal. Water Treat., 216 (2021) 129–139.
[56] K. Laxman, M.T.Z. Myint, M. Al Abri, P. Sathe, S. Dobretsov, J. Dutta, Desalination and disinfection of inland brackish ground water in a capacitive deionization cell using nanoporous activated carbon cloth electrodes, Desalination, 362 (2015) 126–132.
[57] A.G. El-Deen, R.M. Boom, H.Y. Kim, H. Duan, M.B. Chan-Park, J.-H. Choi, Flexible 3D nanoporous graphene for desalination and bio-decontamination of brackish water via asymmetric capacitive deionization, ACS Appl. Mater. Interfaces, 8 (2016) 25313–25325.
[58] M.I. Gil, F. López-Gálvez, S. Andújar, M. Moreno, A. Allende, Disinfection by-products generated by sodium hypochlorite and electrochemical disinfection in different process wash water and fresh-cut products and their reduction by activated carbon, Food Control, 100 (2019) 46–52.
[59] J.M. Martins, S. Majdalani, E. Vitorge, A. Desaunay, A. Navel, V. Guiné, J.F. Daïan, E. Vince, H. Denis, J.P. Gaudet, Role of macropore flow in the transport of *Escherichia coli* cells in undisturbed cores of a brown leached soil, Environ. Sci. Processes Impacts, 15 (2013) 347–356.
[60] J. Marugán, R. van Grieken, C. Pablos, Kinetics and influence of water composition on photocatalytic disinfection and photocatalytic oxidation of pollutants, Environ. Technol., 31 (2010) 1435–1440.
[61] J.L. Del Pozo, M.S. Rouse, J.N. Mandrekar, J.M. Steckelberg, R. Patel, The electricidal effect: reduction of *Staphylococcus* and *Pseudomonas* biofilms by prolonged exposure to low-intensity electrical current, Antimicrob. Agents Chemother., 53 (2009) 41–45.

Supporting information

Table S1
Percentage weight of impurities present in activated carbon material during energy-dispersive X-ray spectroscopy analysis

Element	Percentage weight (wt.%)	Weight percent (wt.% Sigma)	Atomic %
O	82.54	0.49	90.96
Al	1.17	0.19	0.77
Si	3.47	0.18	2.18
S	4.55	0.19	2.50
Cl	3.38	0.19	1.68
Ca	3.16	0.20	1.39
Ni	1.73	0.37	0.52

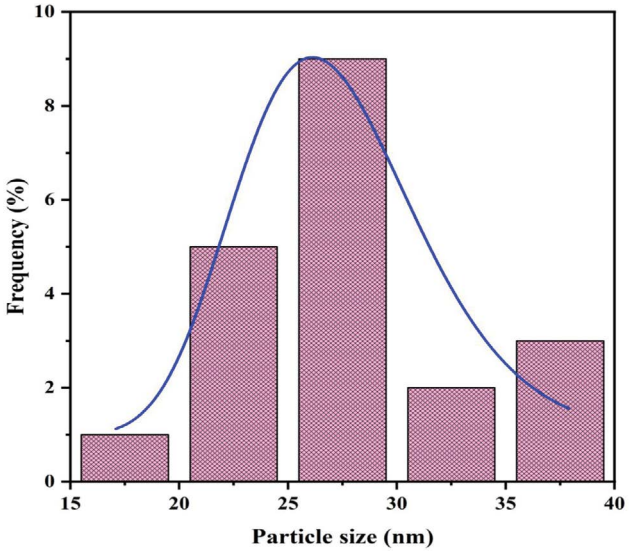

Fig. S1. Histogram of particle-size distribution.

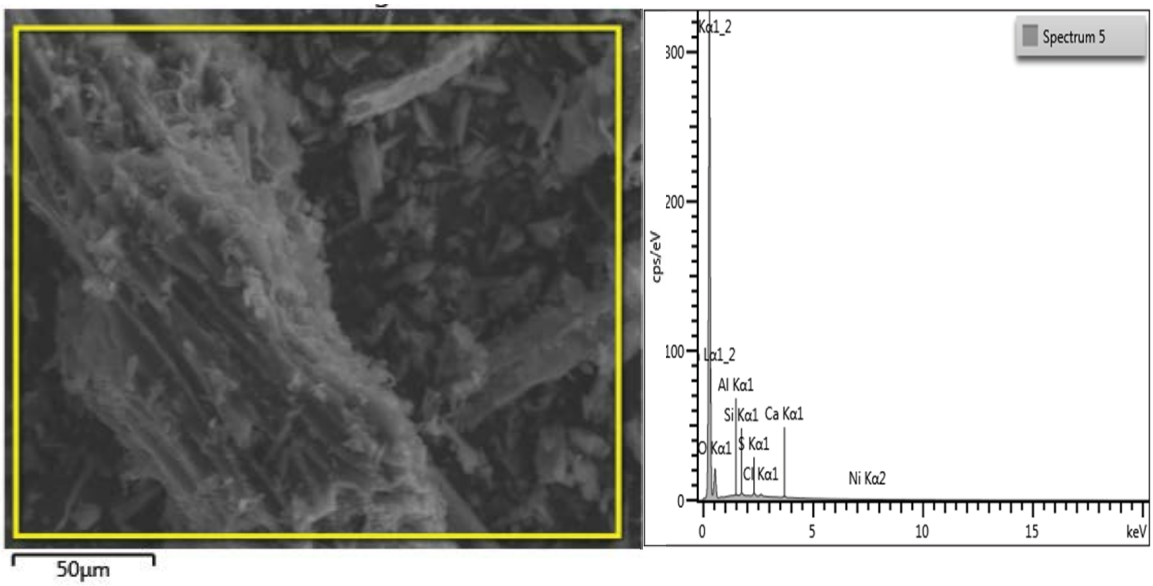

Fig. S2. Energy-dispersive X-ray spectroscopy analysis of activated carbon powder.

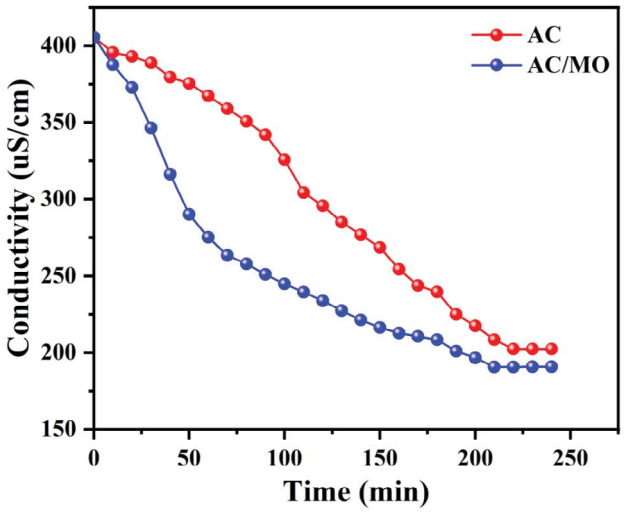

Fig. S3. Conductivity changes with time for activated carbon and AC/MO electrodes during the capacitive deionization process.

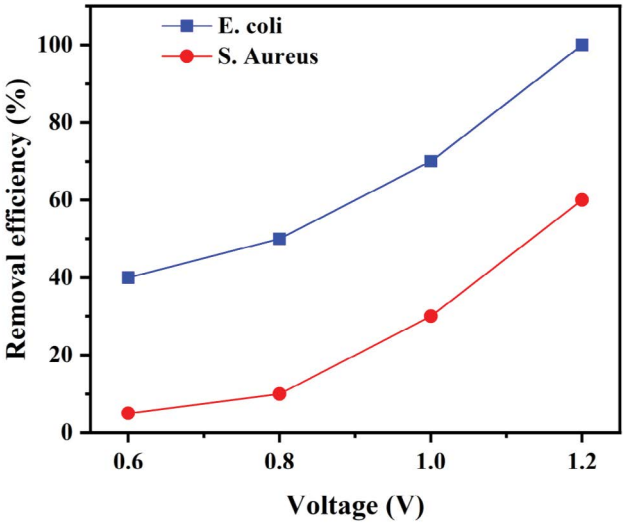

Fig. S5. Effect of applied voltage on bacterial removal during the capacitive deionization process.

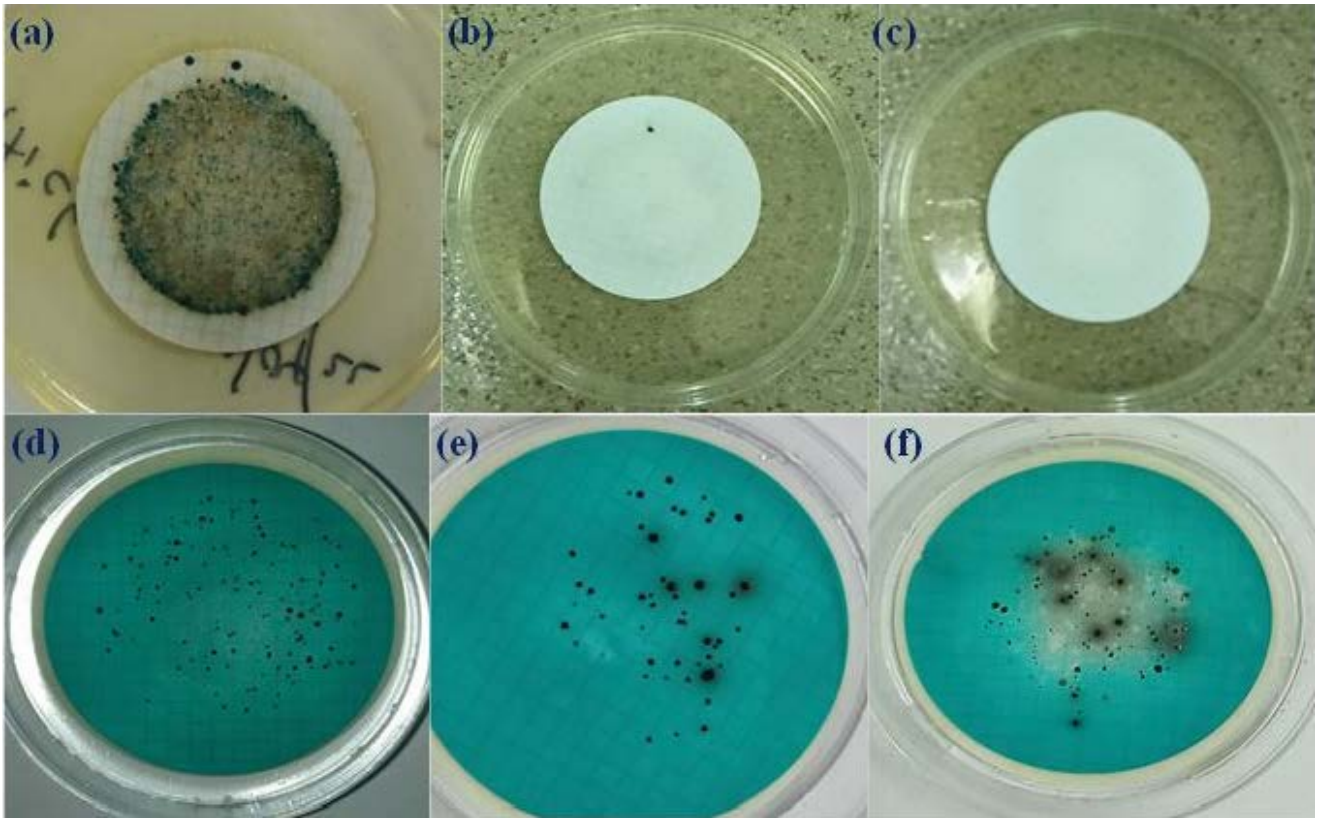

Fig. S4. (a,d) Before treatment, (b,e) after treatment with pure metal oxides for 2 h, (c,f) after treatment with pure metal oxides electrodes after 4 h. (Blue colonies indicating *Escherichia coli* and black colonies indicates *S. aureus* bacteria).